The 13th International Symposium on Fluid Control, Measurement and Visualization
November15-18, 2015, Doha, Qatar
FLUCOME2015

Heat transfer augmentation of MHD duct flow via current injection

A. H. A. Hamid[1, 2, *], W. K. Hussam[1], G. J. Sheard[1]
[1] The Sheard Lab, Department of Mechanical and Aerospace Engineering, Monash University, Victoria 3800, Australia
E-mail: Greg.Sheard@monash.edu
[2] Faculty of Mechanical Engineering, Universiti Teknologi MARA, 40450 Selangor, Malaysia
*Corresponding author, E-mail: hussein@salam.uitm.edu.my

ABSTRACT
In the present study, the idea of heat-transfer enhancement from a duct wall is based on generating the intensive flow vorticity parallel to a magnetic field downstream of a field-aligned cylinder. The electromagnetic effects on the quasi-two-dimensional flows is in the form of Hartmann friction and the forcing due to the injected electric current from a Hartmann wall. The electric current amplitude and frequency are systematically varied to explore its influences on the convective heat transport phenomenon. This investigation builds on a recommendation from previous work dedicated to understand of the flow stability in a similar configuration. The results indicate that the imposed current injection significantly alters the dynamics behavior of the wake behind a cylinder, and that the convective heat transfer improves by almost twofold.

Keywords: *magnetohydrodynamic, heat transfer, vortex shedding*

1. INTRODUCTION
It is known that MHD effects serve to reduce the thermal-hydraulic performance of MHD duct flows by greatly increasing the pressure drop and reducing the heat transfer coefficient through laminarization of the flow. The stabillizing effect derives from the additional damping in the form of Joule dissipation. MHD flows in rectangular ducts, amongst many other geometries, had received most attention in the past due to their wide application [1], especially in the cooling system of poloidal self-cooled blankets. The cooling process can be assisted by mixing of the flow via turbulence or vortical structures. The vortex motion induces significant velocity component in transverse direction and thus improving convective heat transport in this direction.

It has been shown previously that the heat transfer can be further improved by modifying the kinematics of these wake vortices via an active or passive excitation. Hussam *et al.* [2] reported that the optimum perturbations leading to Kármán vortex shedding are localized in the near-wake region around the cylinder, which can be accomplished by a geometric configuration alteration (in passive mode) and by a cylinder oscillation (in active mode). It has been found that increasing oscillation amplitude leads to a higher convective heat transfer from a hot wall [3], thyough the gains become more modest at larger amplitudes [4]. Furthermore, substantial improvement in Nusselt number has been observed when the cylinder oscillates with a frequency within the lock-in regime [5]. An oscillation frequency beyond this lock-in regime leads to a lower convective heat transport [3]. It is also found that higher oscillation amplitude leads to a lower optimum oscillation frequency [4] and broader primary lock-in regime [6].

In general, it can be concluded that the presence of turbulence promoter in the channel improves heat transfer augmentation via transverse fluid mixing and reduced thermal boundary layer thickness. However, studies relevant to channel heat transfer enhancement in an MHD flows are rather scarce.

Furthermore, employing a mechanical actuator for such turbulizers in a duct faces significant technical obstacles to a practical implementation. Alternatively, one can take advantage of the MHD flow characteristics, i.e. the presence of an imposed magnetic field in an electrically conducting flow, to intensify vortical structures by means of electric current injection, either from an electrode mounted flush with one of the Hartmann walls, or from the conducting cylinder. The design and implementation of such a system would be more practical and simpler as compared to a mechanically actuated turbulence promoter system. This idea has been already used by [7] to generate vortices parallel to the imposed magnetic field, but not yet in a duct arrangement with side-wall heating. The present work investigates the heat transfer, pressure drop and efficiency enhancement for the cylinder wake flows with a current injection vortex augmentation. We are particularly interested in a flow with Reynolds number Re = 1500 and Hartmann number Ha = 500 in a duct with a blockage ratio β = 0.2. Owing to the fact that there is a limited number of studies on an actively excited cylinder wake vortices in an MHD duct flow in the literature, the present investigation is anticipated to furnish valuable information for the design of efficient heat transport systems in high-magnetic-field applications.

2. NUMERICAL METHOD AND VALIDATION

In the current investigation a flow of electrically conducting fluid passing over a circular cylinder placed in the center of the duct is considered (as depicted in Fig. 1). The bottom wall of the duct is uniformly heated. A constant uniform magnetic field is imposed in the axial direction. The wake flow is modified by means of current injection through the cylinder. A quasi-two-dimensional (quasi-2D) model for MHD duct flow [8] is employed. Generally the SM82 model is applicable for MHD duct flows under the influence of a strong transverse magnetic field, although some deviation from quasi-2D behavior can be observed in some situations, e.g. in complex geometry ducts. Under the SM82 model the non-dimensional magnetohydrodynamic equations of continuity, momentum and energy reduce to

$$\nabla \cdot \mathbf{u} = 0, \tag{1}$$

$$\frac{\partial \mathbf{u}}{\partial t} = -(\mathbf{u} \cdot \nabla)\mathbf{u} - \nabla p + \frac{1}{Re_L}\nabla^2 \mathbf{u} + \frac{H}{Re_L}(\mathbf{u}_0 - n\mathbf{u}), \tag{2}$$

and

$$\frac{\partial \theta}{\partial t} + (\mathbf{u} \cdot \nabla) = \frac{1}{Pe}\nabla^2 \theta, \tag{3}$$

respectively. $\mathbf{u}$, p and θ are the velocity, pressure and temperature fields, respectively, projected onto a plane orthogonal to the magnetic field, ∇ is the gradient operator and $\mathbf{u}_0$ is the force vector field. The dimensionless parameters Reynolds number, Hartmann number and Peclet number are defined as $Re_L = U_0 L/\nu$, $Ha = Ba\sqrt{\sigma/\rho\nu}$ and $Pe = U_0 L/k = Re_L Pr$, where L is half duct width, U_0 is peak inlet velocity, B is imposed magnetic field, a is out-of-plane duct depth, σ, ρ, ν and k are magnetic permeability, density, kinematic viscosity and thermal conductivity of the liquid metal, respectively. Here length is scaled by L, velocity by U_0, pressure by ρU_0^2, time by L/U_0 and temperature by the temperature difference between the bottom and top walls, $\Delta\theta$.

In the momentum equation, the force vector field $\mathbf{u}_0$ is defined as $\mathbf{u}_0 = \mathbf{j} \times \mathbf{e}_z = \nabla\psi_0 \times \mathbf{e}_z$, where $\mathbf{j}$ is the electric current density and ψ_0 is the electrical potential. Under a high magnetic field condition, the equations governing continuity of electric current and incompressibility are linear, so they may be averaged to give $\nabla \cdot \mathbf{j} = j_w$, $\mathbf{j} = Ha(\mathbf{E} + \mathbf{u} \times \mathbf{e}_z)$ and $\nabla \cdot u = 0$. Here j_w is the current density injected at one or both of the confining planes, and $\mathbf{E}$ is a dimensionless electrical field. The z-averaged current can be expressed as the gradient of a scalar ψ_0 satisfying a Poisson equation with the source term being j_w as $\mathbf{j} = \nabla\psi_0$ and $\nabla^2 \cdot \psi_0 = -j_w$.

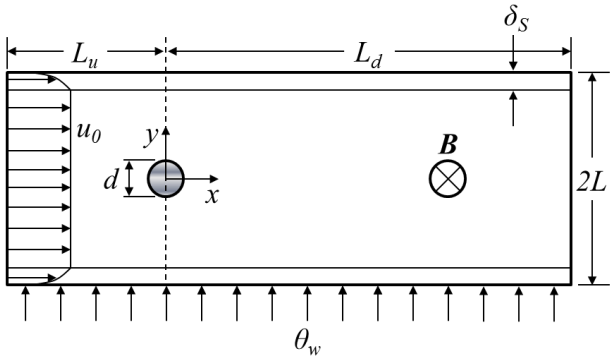

Figure 1: Schematic diagram of the system under investigation. The shaded circle indicates a cylinder of infinite extension along the *z*-axis with diameter *d*.

This Poisson equation is first solved for a source term at the current injection point that is a Dirac function located at $\mathrm{O} = (0, d)$, i.e. $\Phi(x, y) = j_w(x, y) = I\delta(x, y - d)$, on a domain extending infinitely in streamwise direction and bounded by duct side-walls at $y = 0$ and $y = 2L$. Then, the solution is shifted in the negative-y direction at a distance of L in accordance with the global coordinate system (i.e. zero being at the centre of the duct in the vertical direction). Imposing Neumann condition at the boundaries due to insulating Shercliff walls, i.e. $\partial\psi_0/\partial z = 0$ at $y = -L$ and $y = L$ leads to

$$\psi_0(x, y) = \frac{1}{4\pi}\left[\ln\frac{1}{\cosh(\pi x/2L) - \cos(\pi(y_L - d)/2L)} + \ln\frac{1}{\cosh(\pi x/2L) - \cos(\pi(y_L + d)/2L)}\right]. \tag{4}$$

I is the current amplitude which is non-dimensionalized as $\hat{I} = ILU_0\sqrt{\rho\nu\sigma} = IRe_L\sqrt{\rho\nu^3\sigma}$. The force field is then given by

$$\mathbf{u}_0 = \nabla\psi_0 \times \mathbf{e}_z = \left\langle \frac{\partial\psi_0}{\partial x}, \frac{\partial\psi_0}{\partial y}, 0 \right\rangle \times \mathbf{e}_z. \tag{5}$$

The electric current is injected from the cylinder in pulses with various amplitude, I, and angular frequency, $\omega_f = 2\pi f_f$, where f_f is the forcing frequency. The pulse width τ/T is fixed at $\tau/T = 0.25$, where T is the period of the current oscillation. The time averaged Nusselt number is quantified by

$$Nu = \frac{1}{L_w}\int_0^{L_w} \overline{Nu_x}(x)\mathrm{dx}, \tag{6}$$

where L_w is the length of the heated bottom wall and $\overline{Nu_x}$ is the local time-averaged Nusselt number.

An advanced, high-order, in-house solver based on a spectral element method for spatial discretization is employed to simulate the cases. In order to verify the solver, vorticity profiles of quasi-2D MHD duct obtained from the numerical computations are compared with the analytical solution, which is given by $\xi = \partial v/\partial x - \partial u/\partial y = \sqrt{H}\sinh\left(\sqrt{H}\,y\right)/\left(\cosh\left(\sqrt{H}\right) - 1\right)$, where ξ is vorticity. The exact solution for $u(y)$ is given in [9]. Figure 2(a) shows that the results from the numerical computations is in excellent agreement with the analytical solutions. Regression analysis of the data reveal relative standard errors (RSEs - which evaluates the residuals relative to the computed data) of 0.41%, 0.55% and 0.83% for H = 500, 1000 and 2000, respectively. Since the

Shercliff layers have thickness is inversely proportional to the square root of Hartmann number, i.e. $\delta_S = a\,Ha^{-1/2}$ [9], the increased RSE with increasing friction parameter is expected due to the demand for finer resolution at higher *H*. The present solver was further validated by comparing the critical Reynolds number at the onset of vortex shedding from experimental data of Frank *et al.* [10] with the results from the present computations, as shown in Fig. 2(b). A good agreement with published data is found, which again supports the accuracy of the present solver. Further validation of the code can be found in [4].

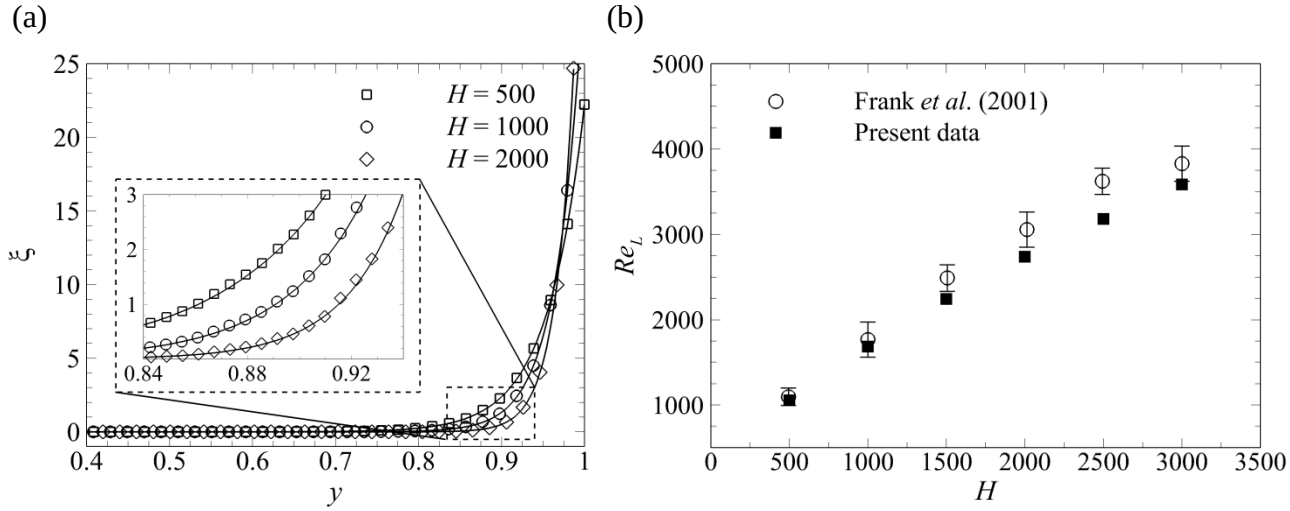

Figure 2: Vorticity profiles of fully developed quasi-2D duct flows in the vicinity of the side wall for *Re* = 3000 and *H* as indicated. Symbols show results from present computations, while solid lines represent the analytical solution of SM82 model. (b) Critical *Re* at the onset of vortex shedding for $\beta = 0.1$ and various magnetic field strength.

A grid independence study has been performed by varying the element polynomial degree from 3 to 11, while keeping the macro element distribution unchanged. The grid consists of four regions: two regions near the transverse walls, a core region, and a region in the vicinity of the cylinder. Small elements are distributed near the walls and the cylinder (as shown in Fig. 3) to resolve the expected high gradients in MHD flows and to capture the crucial characteristics of the boundary layer (e.g. boundary layer separation). The grid is also compressed in the horizontal direction towards the cylinder. The time-averaged Strouhal number (*St*), total drag coefficient (C_D), the integral of velocity magnitude throughout the domain (L_2 norm) and Nusselt number (*Nu*) were monitored, as they are known to be sensitive to the domain size and resolution. Errors relative to the case with highest resolution, $\varepsilon_P = |1 - P_{N=11}|$, were defined as a monitor for each case, where *P* is the monitored parameter. A demanding MHD case with *H* = 500, Re_L = 1500, *I* = 60, ω_f = 4 and $\tau/T = 0.25$ was chosen for the test. The results are presented in Table 1, and show rapid convergence when the polynomial order increases. A mesh with polynomial degree 8 achieves at most a 0.9% error and is therefore used hereafter.

Table 1: Grid independence study at *H* = 500, Re_L = 1500, *I* = 60, $\omega_f = 4$ and $\tau/T = 0.25$

N_P	3	4	5	6	7	8	9	10
ε_{St}	0.2813	0.4048	0.3903	0.2714	0.2624	0.1884	0.1698	0.0882
ε_{C_D}	4.4134	0.2138	0.6136	1.1087	1.0248	0.5990	0.9263	0.8289
$\varepsilon_{L_2\,norm}$	0.5788	0.0296	0.1104	0.1812	0.1763	0.1040	0.1095	0.0446
ε_{Nu}	5.0943	3.4334	2.5580	1.9540	1.5904	0.8984	0.5187	0.2656

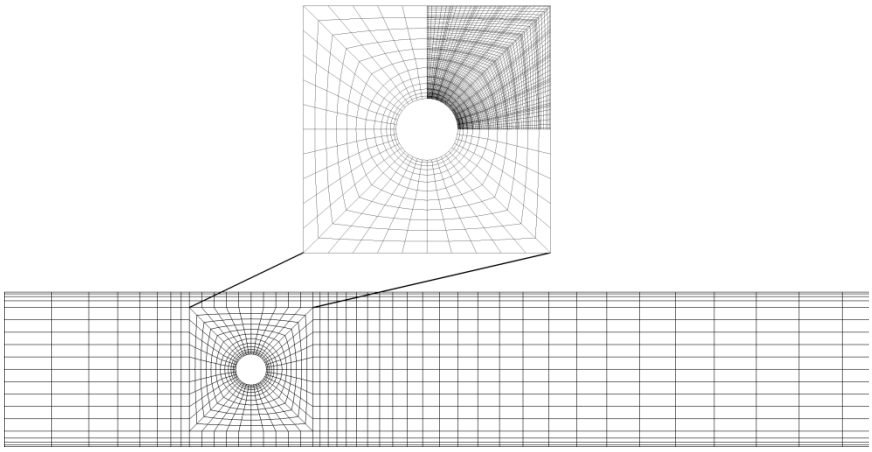

Figure 3: Macro-element distribution of the computational domain, and magnified mesh in the vicinity of the cylinder, with the upper right quadrant representing the spectral element distribution with N_p = 8. The mesh extends 3.2L upstream and 8L downstream.

3. RESULTS AND DISCUSSION

3.1 Effects of the current injection frequency and amplitude on heat transfer

Simulations were carried out to determine the effects of current injection frequency and amplitude on convective heat transfer from a uniformly heated side wall. The forcing frequency was varied between $\omega_f = 0.5$ and 10 for I = 12, 30 and 60. It is observed from Fig. 4 that higher current amplitude leads to a higher Nusselt number for all frequencies. Furthermore, the Nusselt number peaked at $1.3 \le \omega_f \le 1.75$, which corresponds to $0.28 \le F \le 0.36$ within the investigated current amplitude.

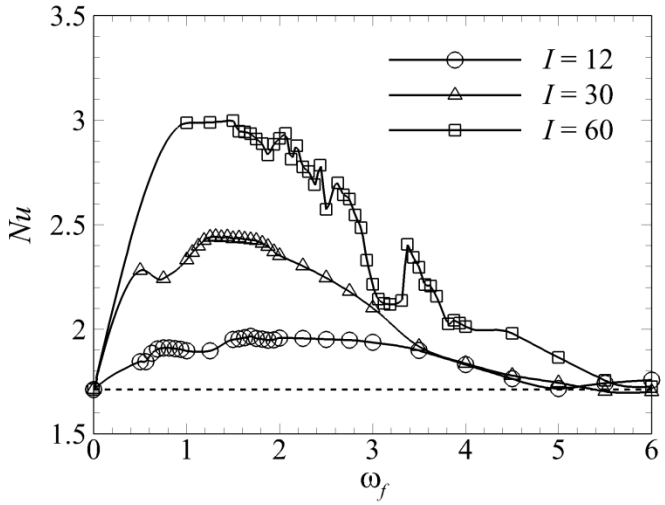

Figure 4: Time-averaged Nusselt number along the downstream of the heated wall plotted against ω_f at I as indicated. The horizontal dashed line denotes the Nusselt number for the basae case (i.e. without current injection).

Spectral analysis of the cylinder lift coefficient reveals that this frequency is appreciably lower than the lock-in frequency range (a state where the vortex shedding is synchronized with the forcing frequency), as shown in Fig. 5. This observation is in disagreement with previous studies of channel heat transfer from a heated wall in the presence of rotationally oscillating cylinder [3] and transversely oscillating cylinder [11], where maximum heat transfer was observed at the lower range of the lock-in frequency. The observed discrepancy between the present results and the previous observations is

attributed to the different mechanism of vorticity supply in both cases. In the oscillating cylinder case, the wake vortices is derived (or enhanced) through the relative motion between the cylinder and the free stream. This type of flow is governed by the relative size of two time scales; the time scales of vortex dynamics and of cylinder oscillation. When the time scales of oscillation is comparable to that of vorticity, the vortex shedding is synchronized with the cylinder oscillation (the oscillation frequency is said to be in lock-in regime). This leads to a generation of high intensity vortices and a substantial interaction between the vortices and the channel walls [3]. On the other hand, if the time scales of the oscillation is much lower or much higher compared to the vortex dynamics (i.e. forcing frequency in the unlock-in regime), the rate at which vorticity is shed into a wake is governed by the natural frequency irrespective of the oscillation frequency. The downstream wake in this state is similar to that for a fixed cylinder [6], and therefore inherit its poor heat transfer characteristic.

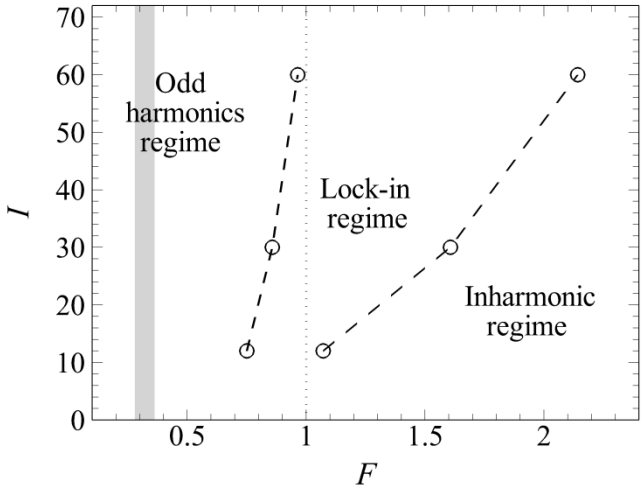

Figure 5: Limits of the lock-in regime as a function of forcing amplitude and frequency. Regime to the left (right) of the lower (upper) bound represent wakes with odd harmonics (inharmonic) in cylinder lift force. The dotted line represent $F = f_f / f_0 = 1$, and the shaded region highlights the zone where *Nu* is maximum.

In the present case, however, the wake vortices are governed by the forcing current injection, which is indicated by the presence of strong narrow peaks at the forcing frequency and its harmonics in the spectra of lift coefficient (which is shown in Section 3.2). For a low forcing frequency, the amount of vorticity supplied to each shed vortex is large, which leads to a large wake vortical sturcture (as shown in Fig. 6). This in turn would generally enhance the wake-boundary layer interaction, and thus the heat transfer from the side wall. However, a lower forcing frequency also means less number of shed vortices for a given time duration, which may not be beneficial for the heat transfer enhancement. The competition between the role of size and number of the shed vortices results in a non-monotonic trend of the $Nu - \omega_f$ relation.

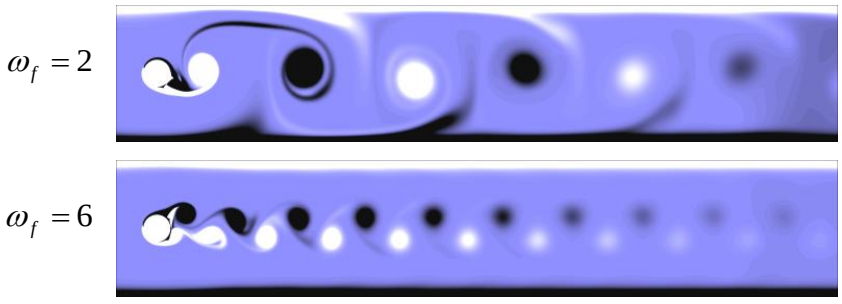

Figure 6: Contour plots of vorticity for *I* = 30. Contour levels ranges between -2 and 2, with light and dark contours represent negative and positive vorticity, respectively.

It is also interesting to observe that at higher frequencies, the Nusselt number tends to asymptote towards the value of a non-forced case (i.e. without current injection). Similar observation has been reported previously for a rotationally oscillating circular cylinder [4] and a transversely oscillating square cylinder [12]. This observation can be attributed to the fact that for a high forcing frequency, the amount of vorticity feeding into the wake per shedding cycle decreases. This leads to a more coherent and smaller wake structure, resembling the ideal Kármán vortex shedding. The vortices are aligned closer to the duct centerline, which is accompanied by a diminishing effect of interaction between wake vortices and thermal boundary layers (as shown in Fig. 6).

It is also worth mentioning that, the fluctuation trend in Nusselt number for a higher forcing amplitude is due to the different modes of response at different forcing frequencies. For example, increasing forcing frequency from $\omega_f = 3.3125$ to 3.375 at $I = 60$ leads to an abrupt increase in Nu (i.e. by 13%). Examination of vorticity contours for $\omega_f = 3.375$ reveals that there is a substantial interaction between wake vortices and the heated wall due to the broadening of a wake width (as shown in Fig. 7(a)). There is clear evidence of the boundary layer entrainment from the heated wall into the wake, as well as strong mixing between the high-temperature fluid near the heated region with the low-temperature core flow. In the case with $\omega_f = 3.3125$, however, almost no boundary layer entrainment from the heated wall into the wake was observed (as can be seen in Fig. 7(b)), results in poor mixing between the hot fluid near the boundary and cold fluid in the core flow, which explains the abrupt increase in Nusselt number at this particular forcing frequency. However, this observation may be associated with limited numerical precision, in which further justification is worth doing in the future.

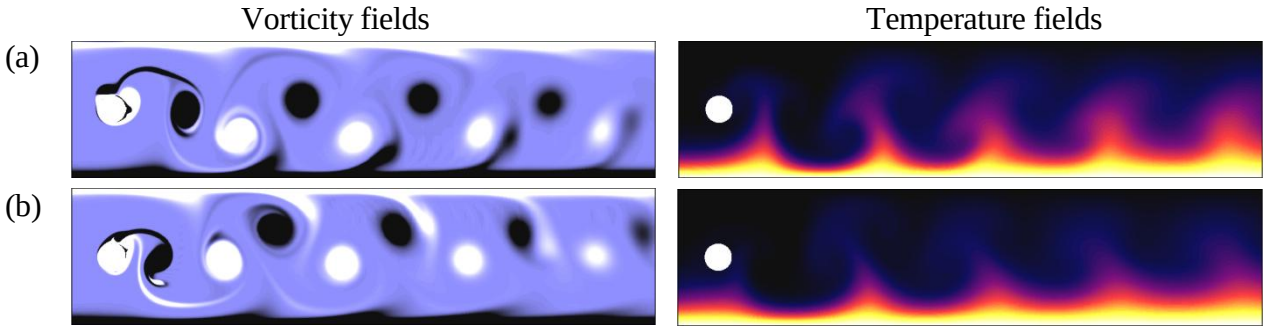

Figure 7: Instantaneous vorticity contour plots for $I = 60$ and (a) $\omega_f = 3.375$ and (b) $\omega_f = 3.3125$. Vorticity fields: contour levels are as per Fig. 4. Temperature fields: dark and light contours show cold and hot fluid, respectively.

3.2 Shedding frequency analysis

In this section, a Fourier analysis of the lift coefficient time histories and the vorticity time series is presented in order to investigate the response in the wake of a circular cylinder with a current injection. The analysis was conducted after elimination of transient response. The peaks in the resulting spectra are interpreted in terms of the natural shedding frequency, forcing frequency and their harmonics. The analysis revealed three distinct regimes of wake response, i.e. odd harmonics regime, lock-in regime and inharmonic regime.

In the lock-in regime, the wake shedding frequency is governed only by the forcing current. In general, the synchronization of vortex shedding (lock-in state) occurred at $0.8 \le F \le 2$ within the investigated forcing amplitude (refer Fig. 5). This range of synchronization is relatively much broader than previously reported for the transversely oscillating cylinder counterpart, which lies within a frequency band of $0.75 \le F \le 1.25$ for an oscillation displacement of 50% of the cylinder diameter [13]. The reason for the discrepancy is due to the aforementioned different vorticity generation mechanism. It was also observed that higher forcing amplitude leads to broader synchronization range, which is in agreement with the previous findings [13].

It is also interesting to note that in the present cases, a distinct spectrum was observed in the unlock-in regime compared to the cases with oscillating and vibrating cylinder. The typical lift force history is shown in Fig. 8(a), where it resembles a distorted waveform. When the forcing frequency is

below the lock-in frequency threshold (i.e. in the region to the left of the lower bound shown in Fig. 5), the spectrum composed of forcing frequency and its odd harmonics (as shown in Fig. 8(c) for $\omega_f = 1$). Beyond the lock-in regime (i.e. the inharmonic regime shown in Fig. 5), the forcing frequency, its harmonic(s) and fraction of the natural shedding frequency (i.e. $f = nf_0/4$, where n are odd integers) are present in the spectrum (as shown in Fig. 8(c) for $\omega_f = 6$). The presence of multiple peaks are a results of complex interaction between the forcing excited vortices and the naturally produced one. It has been shown previously, however, that only the natural shedding frequency and forcing frequency are dominant in the unlock-in regime for oscillating cylinder [14], and that only the natural shedding frequency is dominant in the unlock-in regime for vibrating cylinder [15]. In the lock-in regime, the spectrum is typical; the lift force fluctuation synchronizes with the forcing frequency (shown by the strong narrow peak at $f/f_f = 1$ in Fig. 8(c) for $\omega_f = 3.5$) and with nearly uniform amplitude (as shown in Fig. 8(b)).

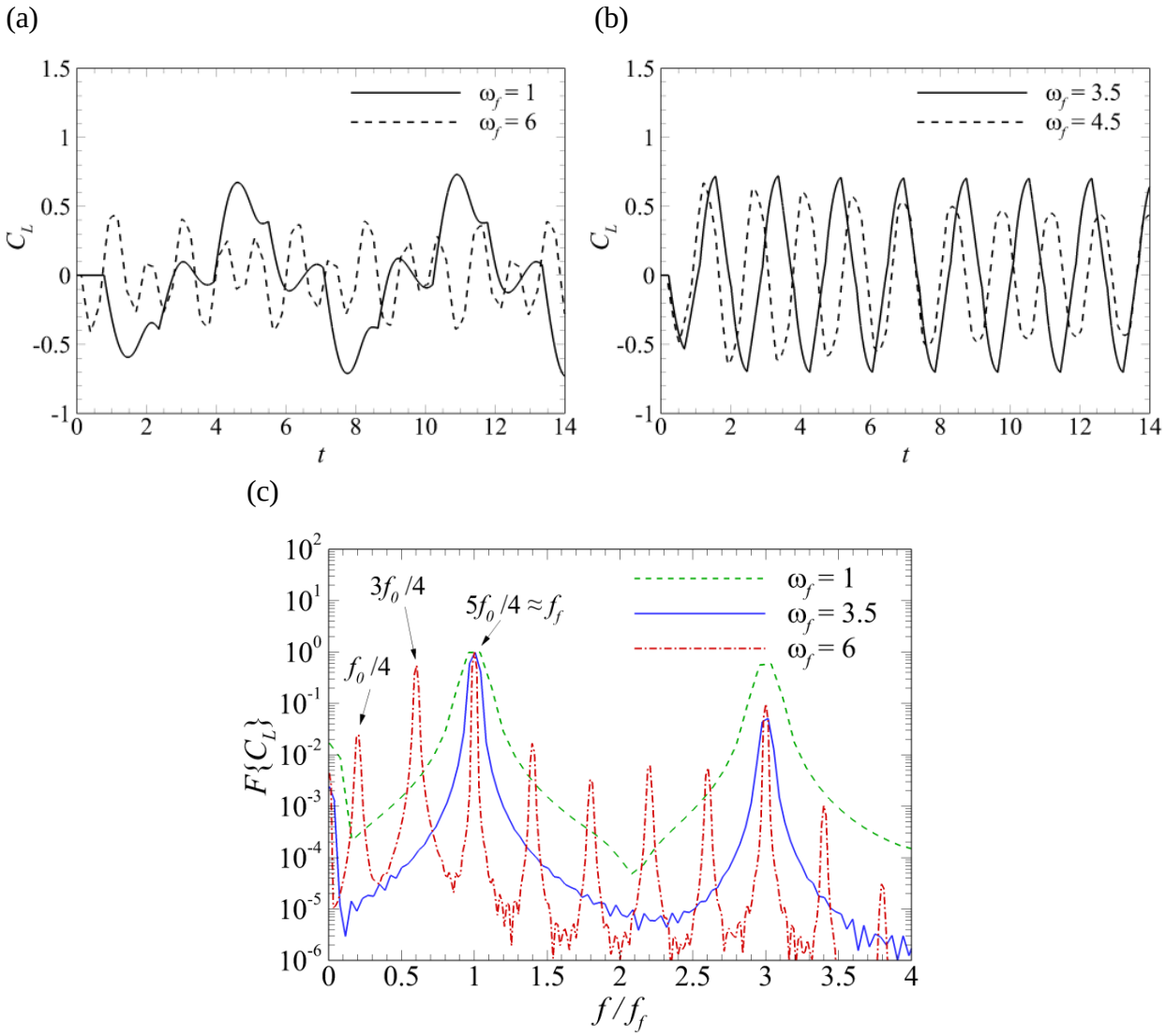

Figure 8: A typical time variation of the cylinder lift coefficient at I = 12 and ω_f as indicated for (a) unlock-in regimes and (b) lock-in regimes.

4. CONCLUSIONS

The present study has investigated the characteristics of MHD flow and heat transfer enhancement by means of wakes behind a cylinder, with current injection as a mean to intensify the vortical structures. The results indicate that on average, Nusselt number increased by 20-80% for ducts with current injection, and is highly dependant on the current injection amplitude and frequency. The Nusselt number peaked at $0.28 \le F \le 0.36$, a range which is appreciably lower than the lock-in frequency range. Shedding frequency analysis also reveals a distinct spectrum of cylinder lift coefficient iin the unlock-in regime.

ACKNOWLEDGEMENT

This research was supported by the Australian Research Council through Discovery Grants DP120100153 and DP150102920, high-performance computing time allocations from the National Computational Infrastructure (NCI), which is supported by the Australian Government, the Victorian Life Sciences Computation Initiative (VLSCI), and the Monash SunGRID. A. H. A. H. is supported by the Malaysia Ministry of Education and the Universiti Teknologi MARA, Malaysia.

REFERENCES

[1] J. Hunt and K. Stewartson, "Magnetohydrodynamic flow in rectangular ducts. II," *Journal of Fluid Mechanics,* vol. 23, pp. 563-581, 1965.

[2] W. K. Hussam, M. C. Thompson, and G. J. Sheard, "Optimal transient disturbances behind a circular cylinder in a quasi-two-dimensional magnetohydrodynamic duct flow," *Physics of Fluids (1994-present),* vol. 24, p. 024105, 2012.

[3] A. Beskok, M. Raisee, B. Celik, B. Yagiz, and M. Cheraghi, "Heat transfer enhancement in a straight channel via a rotationally oscillating adiabatic cylinder," *International Journal of Thermal Sciences,* vol. 58, pp. 61-69, 2012.

[4] W. K. Hussam, M. C. Thompson, and G. J. Sheard, "Enhancing heat transfer in a high Hartmann number magnetohydrodynamic channel flow via torsional oscillation of a cylindrical obstacle," *Physics of Fluids (1994-present),* vol. 24, p. 113601, 2012.

[5] W.-S. Fu and B.-H. Tong, "Numerical investigation of heat transfer characteristics of the heated blocks in the channel with a transversely oscillating cylinder," *International Journal of Heat and Mass Transfer,* vol. 47, pp. 341-351, 2004.

[6] F. Mahfouz and H. Badr, "Forced convection from a rotationally oscillating cylinder placed in a uniform stream," *International Journal of Heat and Mass Transfer,* vol. 43, pp. 3093-3104, 2000.

[7] A. Pothérat and R. Klein, "Why, how and when MHD turbulence at low becomes three-dimensional," *Journal of Fluid Mechanics,* vol. 761, pp. 168-205, 2014.

[8] J. Sommeria and R. Moreau, "Why, how, and when, MHD turbulence becomes two-dimensional," *Journal of Fluid Mechanics,* vol. 118, pp. 507-518, 1982.

[9] A. Pothérat, "Quasi-two-dimensional perturbations in duct flows under transverse magnetic field," *Physics of Fluids,* vol. 19, p. 074104, 2007.

[10] M. Frank, L. Barleon, and U. Müller, "Visual analysis of two-dimensional magnetohydrodynamics," *Physics of Fluids,* vol. 13, p. 2287, 2001.

[11] B. Celik, M. Raisee, and A. Beskok, "Heat transfer enhancement in a slot channel via a transversely oscillating adiabatic circular cylinder," *International Journal of Heat and Mass Transfer,* vol. 53, pp. 626-634, 2010.

[12] S.-J. Yang, "Numerical study of heat transfer enhancement in a channel flow using an oscillating vortex generator," *Heat and mass transfer,* vol. 39, pp. 257-265, 2003.

[13] G. Koopmann, "The vortex wakes of vibrating cylinders at low Reynolds numbers," *Journal of Fluid Mechanics,* vol. 28, pp. 501-512, 1967.

[14] B. Celik, U. Akdag, S. Gunes, and A. Beskok, "Flow past an oscillating circular cylinder in a channel with an upstream splitter plate," *Physics of Fluids,* vol. 20, p. 103603, 2008.

[15] G. E. Karniadakis and G. S. Triantafyllou, "Frequency selection and asymptotic states in laminar wakes," *Journal of Fluid Mechanics,* vol. 199, pp. 441-469, 1989.